A Novel Three-Dimensional Network Containing Pr(III) Ions and Tartrate: Synthesis, Spectroscopic, Thermal, Ab Initio X-ray Powder Structure Analyses, and Photoluminescence Properties

Swastik Mondal,[†] Monika Mukherjee,*,[†] Santu Chakraborty,[‡] and Alok K. Mukherjee[‡]

Department of Solid State Physics, Indian Association for the Cultivation of Science, Jadavpur, Kolkata-700032, India, Department of Physics, Jadavpur University, Kolkata-700032, India

ABSTRACT: A new praseodymium tartrate $[Pr(C_4H_4O_6)(C_4H_5O_6)(H_2O)]$ has been synthesized under hydrothermal conditions and investigated by UV−Vis, FTIR, X-ray powder diffraction, thermal and photoluminescence analyses. The compound crystallizes in the orthorhombic system with $a = 21.973(4)$, $b = 7.587(1)$, $c = 5.958(1)$ Å, space group $P2_12_12_1$, and $Z = 4$. The crystal structure has been solved from laboratory X-ray powder diffraction data using a direct space global optimization technique and refined by the Rietveld method. The Pr atoms in the complex have 9-fold coordination with respect to the oxygens, with the metal center in a distorted monocapped square antiprism coordination. The molecular structure of the complex reveals 22-membered $(Pr_4C_{10}O_8)$ nanosized rectangular motifs assembled into helical chains, which are further linked via carboxylate groups of the tartrate ligands forming a novel three-dimensional polymeric framework. A X-ray powder pattern of the anhydrous praseodymium tartrate obtained by heating the title compound at 230 °C revealed a monoclinic unit cell with $a = 10.964(3)$, $b = 11.612(2)$, $c = 10.456(4)$ Å, $\beta = 108.96(2)°$. The luminescence spectra of the hydrated Pr complex exhibit a signal at 645 nm due to a $^3P_0 \rightarrow {}^3F_2$ transition.

Introduction

Coordination complexes of multifunctional organic ligands have attracted considerable attention in recent years due to their role as possible building blocks of novel framework architectures.[1,2] Depending on the conformation of carbon chains, the end functional groups of organic ligands, and the type of metal ions, a variety of coordination polymers with intriguing topological structures, such as one-dimensional (1D) chains,[3] two-dimensional (2D) grids,[4] three-dimensional (3D) porous motifs,[5] and helical strands[6] can be obtained. The variable and high coordination numbers of trivalent lathanide ions and the small energy difference between various coordination geometries showing a low stereochemical preference make rational design for the self-assembly of lanthanide complexes with potential applications in catalysis, adsorption, and luminescence quite challenging.[7−8]

The polymeric structures of several malonate,[9] succinate,[10] and pyridinedicarboxylate[7] complexes containing lanthanide-(III) metal centers have been established by single crystal X-ray analyses. In this context, tartrate ligands due to their conformational flexibility, ability to behave as completely or partially deprotonated, and diversity in complexing behavior appear interesting for studying the self-assembled molecular network. Although single-crystal X-ray structure analyses of several transition metal tartrates have been reported,[11−12] the structural characterization of lanthanide tartrates is limited to samarium tartrate trihydrate,[13] europium tartrate tetrahydrate,[14] and erbium tartrate trihydrate.[15]

In view of the fact that many important materials including several lanthanide tartrates can be prepared only as microcrystalline powders, X-ray diffraction data collected from crystalline powders are the primary source of structural information. Although single crystal and powder diffraction patterns contain the same intrinsic information, in the former case this information is distributed in 3D space, whereas in the latter case the 3D diffraction data are compressed into one dimension, which leads to considerable overlap of peaks in the powder diffraction pattern. The inability to extract intensities unambiguously for a sufficiently large number of reflections generally prohibits the application of reciprocal-space methods (Patterson and Direct methods) for ab initio structure solution of moderately complex systems. Recent developments in the direct space approaches as implemented in the software packages FOX,[16] DASH,[17] EAGER,[18] where trial structures are generated in direct space and optimized against the experimental profile,[19,20] have shown considerable promise for structure solutions from powder diffraction data.[21] Crystal structures of several metallo−organic complexes using powder X-ray diffraction data have been determined following the direct space methodology.[22,23]

In the present paper, we describe the synthesis, spectroscopic characterization, and crystal structure of a novel praseodymium-(III) tartrate, $[Pr(C_4H_4O_6)(C_4H_5O_6)(H_2O)]$, from X-ray powder data as well as its thermal behavior and luminescence properties.

Experimental Section

Materials and Physical Measurements. All reagents were of AR grade (Aldrich) and used as purchased. The elemental contents (Pr, C, and O) were obtained from an air-hydrolyzed and gently dried sample, by use of a scanning electron microscope (JEOL JSM-6700F) with an energy-dispersive X-ray spectrum analyzer. UV−Vis and IR spectra (as KBr disk) were obtained at ambient temperature with Shimadzu UV-2401 PC, FTIR-8300 spectrometers. Room temperature magnetic susceptibility was measured using an EG and G (USA, model 155) vibrating sample magnetometer. The luminescence measurements with excitation at 590, 490, and 270 nm were recorded in solid state at room temperature using a Hitachi F-4500 spectrofluorimeter. Thermogravimetric and differential scanning calorimetric analyses (TG-DSC) were carried out with a Perkin-Elmer Diamond TG/DTA thermobalance (model N5350030) under a flow of nitrogen (50 mL/min) from 40 to 950 °C at 5 °C min⁻¹.

Synthesis. An aqueous solution (10 mL) of disodium tartrate (0.294 g, 1.5 mmol) was added to an aqueous solution (5 mL) of praseodymium chloride hexahydrate (0.355 g, 1 mmol). A hydrothermal reaction of the resulting mixture was carried out at 170 °C for 24 h. On cooling

* To whom correspondence should be addressed. E-mail: sspmm@iacs.res.in.
† Indian Association for the Cultivation of Science.
‡ Jadavpur University.

Table 1. Comparison of Crystallographic Parameters of Different Metal Tartrates

compound	space group	Z	cell volume ($Å^3$)
$[Pb(C_4H_4O_6)]$[11]	$P2_12_12_1$	4	590.7
$[Sm(C_4H_4O_6)(C_4H_3O_6)]3H_2O$[13]	$P4_12_12$	4	1371.6
$[Er(C_4H_4O_6)]3H_2O$[15]	$P4_12_12$	4	1309.4
$[Y(C_4H_4O_6)(C_4H_5O_6)]2.5H_2O$[35]	$P4_12_12_1$	4	1315.5
$[Pr(C_4H_4O_6)(C_4H_5O_6)]H_2O$ (present work)	$P2_12_12_1$	4	993.1

the reaction product to room temperature (27 °C) overnight, a green compound (praseodymium tartrate) was isolated, which was washed thoroughly with water–ethanol (1:1) and dried (yield ∼ 80%). The elemental analysis by SEM-EDS gave the following results: Pr, 25.54%, C, 29.64%, O, 44.82%. These values compare well with those calculated from the proposed formula $[Pr(C_4H_4O_6)(C_4H_5O_6)(H_2O)]$.

X-ray Powder Data Collection. X-ray powder diffraction data were collected in a Bruker D8 Advance powder diffractometer using monochromatic Cu Kα1 radiation (λ = 1.5406 Å) selected with an incident beam germanium monochromator. The diffraction pattern was scanned with a step length of 0.02° (2θ) and counting time 25 s^{-1} over an angular range 6–100° (2θ) using the Bragg–Brentano geometry. To minimize the preferred orientation effect, the powder material was mounted in a top-loaded sample holder. The stability of the X-ray source and sample was checked by recording the first line of the diffraction pattern after data collection.

Indexing. The first 20 peaks of the powder pattern in the 2θ range 8–30° were fitted using the program TOPAS,[24] and the refined 2θ positions were input into the auto-indexing program DICVOL91.[25] The solution with high figure of merit [M (20) = 21.7; F(20) = 43.0(0.013, 31)][26,27] indexed all peaks in an orthorhombic unit cell having a = 21.970(3), b = 7.586(1), and c = 5.956(1) Å. The results of indexing with the programs NTREOR,[28] TREOR,[29] and ITO[30] also indicated the same orthorhombic solution.

Structure Solution and Refinement. The unequivocal determination of space group using powder diffraction data is not straightforward, and usually more than one space group may be compatible with the diffraction profile. Additional problems may arise for space groups containing only screw axes since the number of reflections extracted from the powder pattern obeying the extinction rule of a screw axis is often quite small. The probabilistic approach[31] as incorporated in EXPO2004[32] provides a quantitative basis for determining the possible extinction symbols from the experimental powder data. The full pattern decomposition was performed with EXPO2004 according to the Le Bail algorithm[33] using a split-type pseudo-Voigt peak profile function[34] in the space group $P2/m\ 2/m\ 2/m$, the Laue symmetry corresponding to the orthorhombic system. Analysis of the powder pattern revealed possible extinction symbols as P_nn, $P\_\_n$, and $P2_12_12_1$. When the pseudotranslation symmetry option was applied in the FINDSPACE module of EXPO2004, the most likely extinction group indicated was $P2_12_12_1$. A comparison of cell volume (V) of the praseodymium complex with those of other metal tartrates (Table 1) indicates that the asymmetric unit of the title compound probably contains two tartrate groups per praseodymium atom.

The room temperature (298 K) magnetic susceptibility measurement indicated that the title complex is paramagnetic. The observed μ_{eff} = 3.74 μ_B, based on molecular weight ∼ 456, i.e., each praseodymium atom is associated with two tartrate moieties and one H_2O molecule, is close to that reported for a Pr(III) complex.[36] The structure solution was carried out in space group $P2_12_12_1$ having a general multiplicity of 4, which provided an acceptable calculated density, and it was the most common space group for crystals belonging to the orthorhombic system.

Attempts to solve the structure by Patterson or direct methods using 463 extracted integrated intensities from the powder pattern were not successful. In either case, however, the Pr atom could be located, but positions of C and O atoms leading to a sensible structural motif could not be determined from successive difference Fourier or E-maps. The structure was therefore solved by the global optimization of a structural model in direct space using the program FOX.[16] This attempts to minimize the difference between the observed and the calculated powder intensities by a simulated-annealing approach (in parallel tempering mode) that moves the constituent fragments defining the structure within
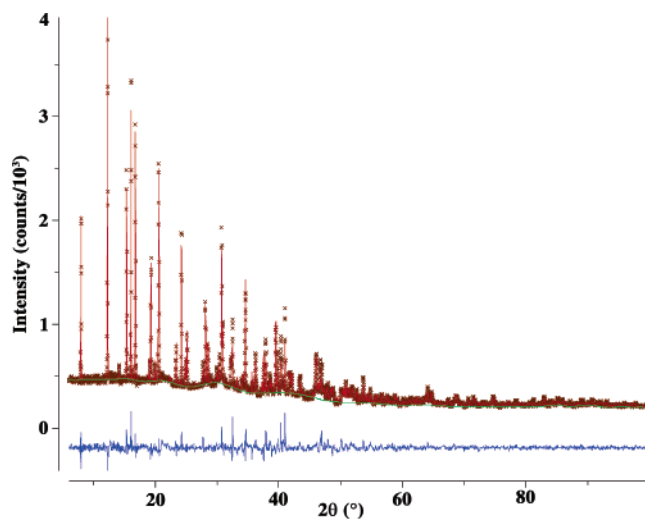
Figure 1. Final observed (crosses), calculated (red line), background (green line), and difference (blue line) profiles for $Pr(C_4H_4O_6)(C_4H_5O_6)$-(H_2O).

the unit cell, varying their positions, orientations, and when appropriate, their conformation.

Lattice and profile parameters, zero-point and interpolated background calculated from previous powder-pattern decomposition based on Le Bail algorithm, were introduced into the program FOX. The tartrate molecular geometry adopted from the standard data incorporated in the MOPAC 5.0 program package,[37] which included the AM1 Hamiltonian,[38] was fully optimized by an energy gradient method. The starting configuration for global optimization of the crystal structure using FOX was obtained by randomly placing one Pr atom, two tartrate moieties with geometry as calculated from an earlier AM1 run, and two water molecules in the unit cell. Bond lengths and bond angles of two tartrate groups were constrained within 0.02 Å and 1.15°, respectively, but the torsion angles were allowed to change. The parallel-tempering algorithm of the program FOX was used for 2θ ranges 6° to 60°. Dynamic occupancy correction option of the program was used to merge excess O atoms of water molecules. After 3 × 10^7 trials, requiring approximately 13 h of computer time on a Pentium IV (512 MB RAM) PC, a solution with R_{wp} = 0.29, χ^2 = 3975, and GOF = 1.53 was obtained. The two water O atoms in the initial model coalesced into a single position.

The atomic coordinates derived from the simulated-annealing procedure of FOX were taken as the starting model of Rietveld refinement with the program GSAS.[39] The refinement was carried out using a 2θ angular range 6.00° to 100.00° with soft constraints on bond distances and angles; the tartrate groups were treated as rigid bodies. It was not necessary to add any constraint regarding the coordination geometry around the praseodymium atom. Hydrogen atoms were placed in calculated positions with C–H and O–H distances restrained to be 0.998 Å. Two isotropic temperature factors, 0.005 Å^2 for the Pr atom and 0.04 Å^2 for the remaining non-H atoms, were refined. The background was described by the Shifted Chebyshev function of first kind with 36 points regularly distributed over the entire 2θ ranges. The peak profiles were fitted with pseudo-Voigt functions using the Thompson-Cox-Hastings formalism.[40] These functions take into account the experimental resolution and peak broadening due to the size and the strain effects. Final Rietveld refinement of 119 parameters (66 coordinates, 3 lattice parameters, 1 preferred orientation parameter, 36 background, 12 profile parameters, 1 scale factor) resulted in conventional agreement factors R_p = 0.0476 and R_{wp} = 0.0638. For the soft constraints, the mean-square deviations to the assigned values were 0.01 Å for bond lengths and 1.0° for bond angles. The agreement between the observed and the calculated patterns was excellent (Figure 1). Relevant crystallographic data are listed in Table 2. The molecular structure, drawn with ORTEP-III,[41] showing the atom numbering is shown in Figure 2. The molecular packing of the complex is given in Figure 4a.
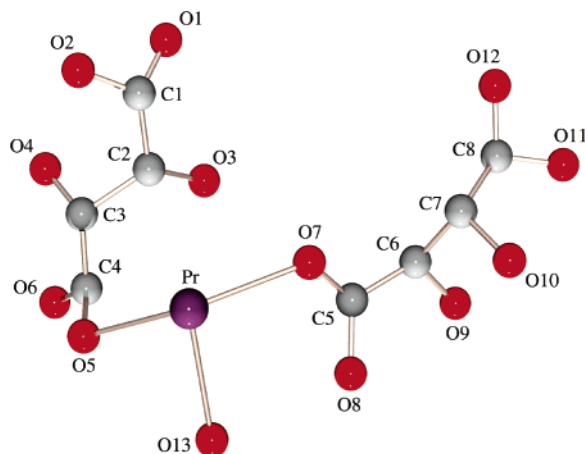
Figure 2. The molecular view of praseodymium tartrate with atom numbering scheme.

Results and Discussion

UV−Vis and IR Spectra. The UV−Vis absorption spectra of solid exhibit three transitions at ca. 446, 472, and 485 nm. The strong band extending from the UV region to ca. 580− 600 nm, assigned as due to Pr^{3+} ions, causes the pale yellow color of the compound. The almost identical UV−Vis spectra reported for trifluoromethanesulfonate and triazocyclohexane complexes of Pr(III)[42] indicate little influence of the ligand environment on the spectra of praseodymium compounds.

In the IR spectrum of the complex, most bands have shifted from their corresponding positions in the free tartaric acid.[43] The disappearance of bands around 1740 cm^{-1} due to ν (C= O) in the free acid suggests deprotonation of the carboxyl groups. The bands appearing at 1604 and 1400 cm^{-1}, respectively, are attributable to the asymmetric and symmetric stretching vibrations of COO$^-$ groups. The value $\Delta\nu = 204$ cm^{-1}, the difference between the two wavenumbers $\nu_{asymm}(COO^-)$ and $\nu_{symm}(COO^-)$, indicates the bridging mode of the carboxylate group.[10] The peak maxima in the fingerprint region (1200− 400 cm^{-1}) are assigned as C−O and C−C stretching and bending (1200−800 cm^{-1}), and Pr−O stretching (433 cm^{-1})
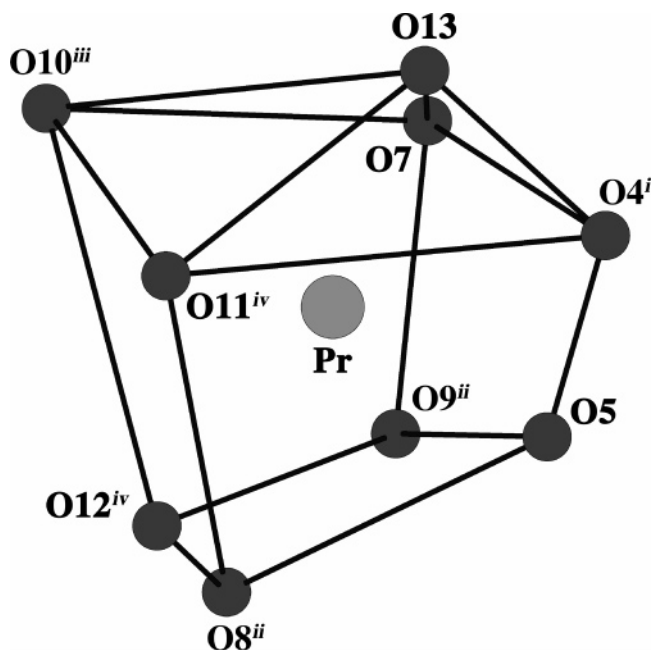

Figure 3. Coordination polyhedron of praseodymium tartrate. Symmetry code: (*i*) 3/2 − *x*, −*y*, 1/2 + *z*; (*ii*) *x*, *y*, *z* − 1; (*iii*) 1 − *x*, *y* − 1/2, 3/2 − *z*; (*iv*) *x*, *y* − 1, *z* − 1.

frequencies.[36] The hydroxyl stretching band with a maximum at 3377 cm^{-1} and a shoulder tailing down to ca. 2980 cm^{-1} indicates extensive intra- and intermolecular hydrogen bonds in the complex.[44] The band due to $\delta(H_2O)$ has been masked within the intense and broad contour of the carboxylate band.

Description of the Structure. Crystal structure determination reveals the composition of the title compound as [Pr(C$_4$H$_4$O$_6$)- (C$_4$H$_5$O$_6$)(H$_2$O)]. Similar to the yttrium, samarium tartrate complexes,[13,35] the asymmetric unit of the praseodymium complex contains one doubly and one singly ionized tartrate ligands necessary for Pr^{3+} charge balance. The metal center in the Pr complex is surrounded by nine oxygen atoms, six of them from the (C$_4$H$_4$O$_6$)$^{2-}$ ligands, two from the (C$_4$H$_5$O$_6$)$^-$ ligands, and one coordinated water molecule. Nine coordinate lanthanide ions have been encountered in some analogous systems in which the ninth coordination of the metal ion is provided by a water molecule.[45,46] As shown in Figure 3, the coordination polyhedron around each praseodymium atom is a distorted monocapped square antiprism.

The Pr−O bond lengths (Table 3) are in the range 2.27(1)− 2.76(1) Å (average value 2.57 Å) with the extreme values corresponding to Pr−O11 (*x*, *y* − 1, *z* − 1) and Pr−O10 (1 − *x*, 1/2 − *y*, 3/2 − *z*) distances, respectively. The O−Pr−O bond angles (Table 3) lie in the range 84.1(13) − 136.4(11)°. These values are similar to those found for nine-coordinated praseodymium cations.[7,9] The average C−O bond distances [1.36 Å] and O−C−O bond angles [111.0°] agree well with those of previously reported lanthanide tartrate complexes.[13,14] Although the H atoms bonded to O atoms could not be reliably located, several intermolecular hydrogen bonds stabilizing the structure were indicated by short O···O contacts (<2.8 Å) and O−H·· ·O angles (>115.0°). These bonds involve the α-hydroxyl O (O3, O10) and carboxylate O (O1, O2, O6, O7, O11) atoms where O3 and O10 atoms act as a single donor [O3···O1 (1/2 − *x*, 2 − *y*, 1/2 + *z*) 1.99 Å, O10···O11 (−*x*, *y* − 1/2, 3/2 − *z*) 2.76 Å], and the O2 atom at (*x*, *y*, *z*) acts as a donor to O6 (1/2 − *x*, 1 − *y*, 1/2 + *z*) [O2···O6 2.14 Å] and O7 (1/2 − *x*, 1 − *y*, 1/2 + *z*) [O2···O7 2.60 Å].
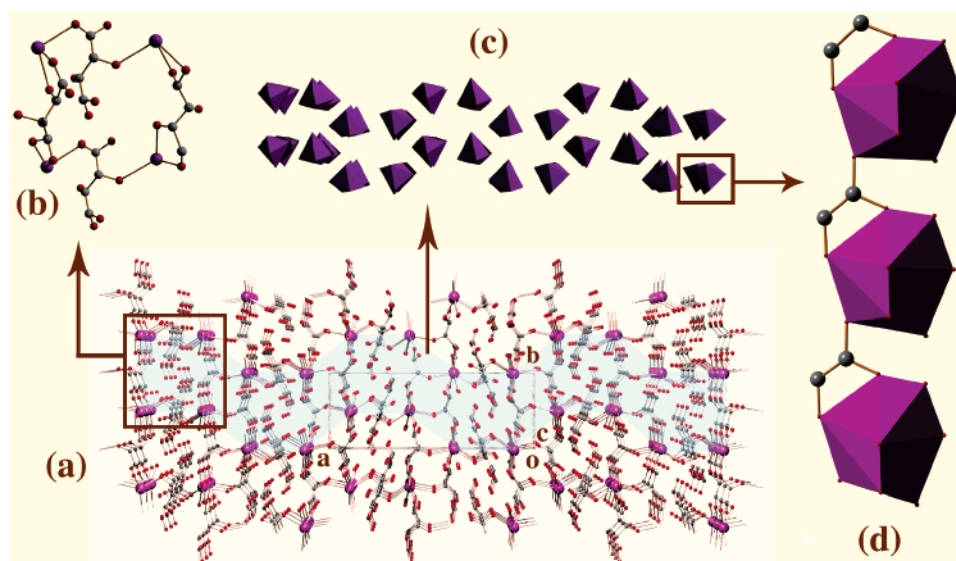
Figure 4. (a) Molecular packing of praseodymium tartrate viewed along the [001] direction. (b) Tetranuclear $Pr_4C_{10}O_8$ motif having 7.59×6.94 Å dimension. (c) Formation of helical chains along the *a*-axis. (d) Linking of successive Pr coordination polyhedron along the *c*-axis.

Table 3. Selected Bond Lengths (Å) and Bond Angles (°)[a]

atoms	bond length	atoms	bond length
Pr–O4[i]	2.74(1)	Pr–O5	2.59(3)
Pr–O7	2.52(2)	Pr–O8[ii]	2.41(3)
Pr–O9[ii]	2.59(2)	Pr–O10[iii]	2.76(1)
Pr–O11[iv]	2.27(1)	Pr–O12[iv]	2.68(4)
Pr–O13	2.62(4)		

atoms	bond angle	atoms	bond angle
O5–Pr–O7	121.7(14)	O5–Pr–O8[ii]	84.1(13)
O5–Pr–O9[ii]	107.7(9)	O5–Pr–O11[iv]	84.6(11)
O7–Pr–O8[ii]	126.7(10)	O7–Pr–O11[iv]	136.4(11)
O7–Pr–O13	89.6(10)	O8–Pr–O11[iv]	86.6(11)
O9[ii]–Pr–O12[iv]	110.3(7)	O12[iv]–Pr–O13	105.4(11)

[a] Symmetry code: (i) $3/2 - x$, $-y$, $1/2 + z$; (ii) x, y, $z - 1$; (iii) $1 - x$, $y - 1/2$, $3/2 - z$; (iv) x, $y - 1$, $z - 1$.

In the structure, two crystallographically independent tartrate ligands act in different fashions. Both the COO^- groups of doubly ionized tartrate moieties link the adjacent metal centers forming infinite parallel chains along the *b*-axis, while the singly ionized tartrate ligand is coordinated to the praseodymium atom via one carboxylate O atom with the other COOH group dangling. The parallel chains are interlinked through α-hydroxyl O atoms leading to a 2D polymeric network (Figure 4a).

The resulting supramolecular structure can be visualized in terms of a simpler planar tetranuclear homometallic rectangular unit with a 22-membered $Pr_4C_{10}O_8$ motif (Figure 4b) having 7.59×6.94 Å dimension. When viewed along the [001] direction, the rectangular building blocks are assembled into helical chains with a period of 21.97 Å running along the *a*-axis (Figure 4c). The successive Pr atoms of in the [001] direction, separated by 5.96 Å, are connected through carboxylate groups, acting like pillars (Figure 4d), creating a novel 3D structure. Interestingly, only a few lanthanide ring-like structures have been reported in the literature, e.g., tetranuclear La and Nd,[47] hexanuclear Sm[48] and Eu,[49] octanuclear La,[50] and decanuclear Dy[51] ring. However, these rings only exhibit isolated molecular structures rather than assembling further into a multidimensional structure. To our knowledge, the only Pr(III) complex forming a rather rare 3D polymeric framework has been structurally characterized recently from single-crystal X-ray analysis.[7]
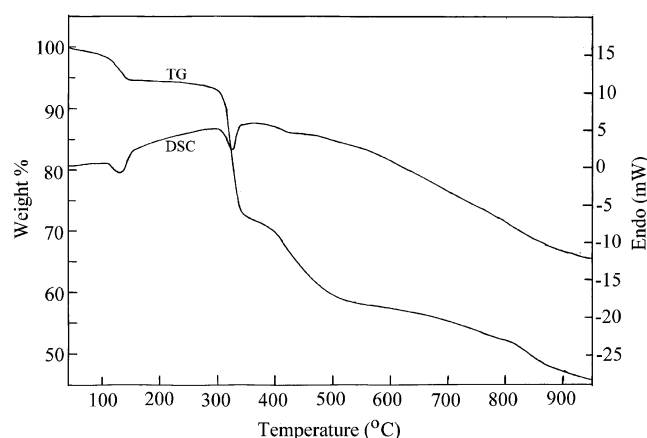

Figure 5. TG-DSC curve for $Pr(C_4H_4O_6)(C_4H_5O_6)(H_2O)$.

Thermal Analysis. The TG-DSC analysis of the title complex (Figure 5) shows three regions of weight loss. The first gradual weight loss between 90° to 160 °C with an endothermic process centered at 131 °C is due to liberation of the coordinated water molecule (theoretical weight loss 4%, observed 4.9%). The temperature for weight loss of a coordinated water molecule is in agreement with those found for other lanthanide compounds described in the literature.[9,52] The second step of weight loss occurs between 285 and 360 °C, and it is an endothermic process (T_{peak}) DSC = 324 °C, followed by the third step between 400° and 530 °C, which is caused by the combustion of part of the organic matter of the organic ligand.[9]

To study the effect of dehydration on the structure of praseodymium tartrate, the title complex was heated at 230 ± 2 °C, the midpoint of the first plateau in the TG curve, in a stream of nitrogen and was kept at the elevated temperature for 30 min. An X-ray powder diffraction pattern (Figure 6) was recorded almost immediately on cooling the compound to room temperature (27 °C), which showed marked changes in comparison with that of the hydrated phase. The resulting single phase of the anhydrous solid was established by indexing of the diffraction pattern on the basis of a monoclinic unit cell with $a = 10.964(3)$, $b = 11.612(2)$, $c = 10.456(4)$ Å, $\beta = 108.96(2)°$; M(20) = 15, F(20) = 24(0.007, 125). Although the structure solution of the anhydrous phase was not attempted
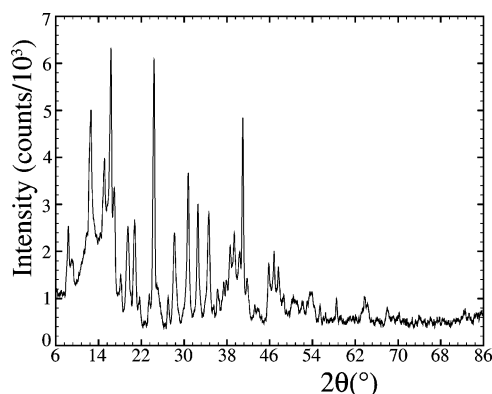
Figure 6. Powder XRD pattern of anhydrous Pr tartrate.

due to the poor quality of the X-ray powder data (average fwhm ∼ 0.30°), it is likely that the loss of water molecules during the dehydration process leaves an empty site in the Pr atom environment, which in turn may induce a different coordination mode of the tartrate ligands. Similar X-ray powder study on structural changes of $La(OH)_2(NO_3) \cdot H_2O$ due to dehydration has been reported earlier.[53]

Photoluminescence Study. The luminescence spectra of Pr-(III) compounds are more complex in comparison to that of other lanthanide(III) systems such as Eu^{3+}, as Pr(III) can show emission lines originating from three different levels ($^3P_0$, $^1D_2$ and $^1G_4$) which span the visible and NIR regions. By comparison with the emission spectra of Pr(III) chelates,[54,55] the signal with maxima at 645 nm in the hydrated Pr(III) complex can be attributed to a $^3P_0 \rightarrow \, ^3F_2$ transition. The fact that we do not observe other transitions that would be expected to originate from a $^3P_0$ level, such as $^3P_0 \rightarrow \, ^3H_4$ at ≈ 490 nm (λ_{exc} = 270 nm) and $^3P_0 \rightarrow \, ^3H_6$ at ≈ 600 nm (λ_{exc} = 490 nm), indicates that the triplet state of the tartrate ligand in the complex is too low to populate the $^3P_0$ level of Pr(III) effectively.

Conclusion

The synthesis, characterization, X-ray powder structure determination, and thermal and photoluminescence behavior of a new praseodymium(III) tartrate complex, $[Pr (C_4H_4O_6)$-$(C_4H_5O_6)(H_2O)]$, have been described. The molecular structure of the complex reveals infinite parallel chains along the *b*-axis. The supramolecular structure containing rectangular $Pr_4C_{10}O_8$ motifs of 7.59 × 6.94 Å dimension shows helical chains of period 21.97 Å running along the *a*-axis. In the [001] direction, the carboxylate groups of the tartrate ligands interlink the helical chains forming a 3D polymeric framework structure. The anhydrous Pr tartrate can be described on the basis of a monoclinic unit cell. To the best of our knowledge, the present work is the second example of a 3D polymeric Pr(III) system and the first report in which the molecular structure of a multidimensional lanthanide tartrate complex has been established from laboratory X-ray powder diffraction data.

Supporting Information Available: Table of atomic coordinates from Rietveld analysis, UV−Vis, FTIR, and photoluminescence data of $[Pr (C_4H_4O_6)(C_4H_5O_6)(H_2O)]$. This material is available free of charge via the Internet at http://pubs.acs.org.

References

(1) Janiak, C. *Dalton Trans.* **2003**, 2781.
(2) Moulton, B.; Zaworotko, M. J. *Chem. Rev.* **2001**, *101*, 1629.
(3) Shin, D. M.; Lee, I. S.; Lee, Y. A.; Chung, Y. K. *Inorg. Chem.* **2003**, *42*, 2977.
(4) Mitsurs, K.; Shimamura, M.; Noro, S. I.; Minakoshi, S.; Asami, A.; Seki, K.; Kitagawa, S. *Chem. Mater.* **2000**, *12*, 1288.
(5) Wang, R.; Gao, E.; Hong, M.; Gao, S.; Luo, J.; Lin, Z. *Inorg. Chem.* **2003**, *42*, 5486.
(6) Wu, C. D.; Lu, C. Z.; Lin, X.; Wu, D. M.; Lu, S. F.; Zhuang, H. H.; Huang, J. S. *Chem. Commun.* **2003**, 1284.
(7) Zhao, B.; Yi, L.; Dai, Y.; Chen, X. Y.; Cheng, P.; Liao, D. Z.; Yan, S. P.; Jiang, Z. H. *Inorg. Chem.* **2005**, *44*, 911.
(8) Spichal, Z.; Necas, M.; Pinkas, J.; Novosad, J. *Inorg. Chem.* **2004**, *43*, 2776.
(9) Hernández-Molina, M.; Lorenzo-Luis, P. A.; López, T.; Ruiz-Pérez, C.; Lloret, F.; Julve, M. *CrystEngComm* **2000**, *31*, 1.
(10) Perles, J.; Iglesias, M.; Ruiz-Valero, C.; Snejko, N. *J. Mater. Chem.* **2004**, *14*, 2683.
(11) De Ridder, D. J. A.; Goubitz, K.; Sonneveld, E. J.; Molleman, W.; Schenk, H. *Acta Crystallogr. C* **2002**, *58*, m596.
(12) González-Silgo, C.; González-Platas, J.; Ruiz-Pérez, C.; López, T. *Acta Crystallogr. C* **1999**, *55*, 740.
(13) Wu, C. D.; Zhan, X. P.; Lu, C. Z.; Lin, X.; Zhuang, H. H.; Huang, J. S. *Acta Crystallogr. E* **2002**, *58*, m228.
(14) Starynowicz, P.; Meyer, G. Z. *Anorg. Allg. Chem.* **2000**, *626*, 2441.
(15) Hawthorne, F. C.; Borys, I.; Ferguson, R. B. *Acta Crystallogr. C* **1983**, *39*, 540.
(16) Favre-Nicolin, V.; Cerný, R. J. *Appl. Crystallogr.* **2002**, *35*, 734.
(17) David, W. I. F.; Shankland, K.; Cole, J.; Maginn, S.; Motherwell, W. D. H.; Taylor, R. *DASH User Manual*; Cambridge Crystallographic Data Centre, Cambridge, UK, 2001.
(18) Harris, K. D. M.; Johnston, R. L.; Albesa Jové, D.; Chao, M. H.; Cheung, E. Y.; Habershon, S.; Kariuki, B. M.; Lanning, O. J.; Tedesco, E.; Turner, G. W. *EAGER*; University of Birmingham, 2001.
(19) Harris, K. D. M.; Tremayne, M.; Lightfoot, P.; Bruce, P. G. *J. Am. Chem. Soc.* **1994**, *116*, 3543.
(20) Tremayne, M.; Kariuki, B. M.; Harris, K. D. M. *Angew. Chem., Int. Ed.* **1997**, *36*, 770.
(21) Harris, K. D. M. *Cryst. Growth Des.* **2003**, *3*, 887.
(22) Zavalij, P. Y.; Yang, S.; Whittingham, M. S. *Acta Crystallogr. B* **2003**, *59*, 753.
(23) Bond, A. D.; Jones, W. *Acta Crystallogr. B* **2003**, *59*, 753.
(24) Coelho, A. A. *J. Appl. Crystallogr.* **2003**, *36*, 86.
(25) Boultif, A.; Louër, D. *J. Appl. Crystallogr.* **1991**, *24*, 987.
(26) De Wolff, P. M. *J. Appl. Crystallogr.* **1968**, *1*, 108.
(27) Smith, G. S.; Snyder, R. L. *J. Appl. Crystallogr.* **1979**, *12*, 60.
(28) Altomare, A.; Giacovazzo, C.; Guagliardi, A.; Moliterni, A. G. G.; Rizzi, R.; Werner, P.-E. *J. Appl. Crystallogr.* **2000**, *33*, 1180.
(29) Werner, P.-E.; Eriksson, L.; Westdahl, M. *J. Appl. Crystallogr.* **1985**, *18*, 367.
(30) Visser, J. W. *J. Appl. Crystallogr.* **1969**, *18*, 367
(31) Altomare, A.; Caliandro, R.; Camalli, M.; Cuocci, C.; da Silva, I.; Giacovazzo, C.; Moliterni, A. G. G.; Spagna, R. *J. Appl. Crystallogr.* **2004**, *37*, 957.
(32) Altomare, A.; Caliandro, R.; Camalli, M.; Cuocci, C.; da Silva, I.; Giacovazzo, C.; Moliterni, A. G. G.; Rizzi, R. *J. Appl. Crystallogr.* **2004**, *37*, 1025.
(33) Le Bail, A.; Duroy, H.; Fourquet, J. L. *Mater. Res. Bull.* **1988**, *23*, 447.
(34) Toraya, H. *J. Appl. Crystallogr.* **1986**, *19*, 440.
(35) Almond, M. J.; Drew, M. G. B.; Morris, S.; Rice, D. A. *Polyhedron* **1996**, *15*, 3377.
(36) Ferenc, W.; Bocian, B.; Walków-Dziewulska, A. *J. Therm. Anal. Calorim.* **2004**, *76*, 179.
(37) Stewart, J. J. P. *MOPAC*, Version 5.0, Quantum Chemistry program exchange 581; Indiana University, 1988.

(38) Dewar, M. J. S.; Zoebisch, E. G.; Healy, E. F.; Stewart, J. J. P. Development and use of quantum mechanical molecular models. *J. Am. Chem. Soc.* **1985**, *107*, 3902−3909.

(39) Larson, A. C.; von Dreele, R. B. *General Structure Analysis System (GSAS)*; Los Alamos National Laboratory Report, LA-UR 86-748; Los Alamos National Laboratory, Los Alamos, NM, 1994.

(40) Thompson, P.; Cox, D. E.; Hastings, J. B. *J. Appl. Crystallogr.* **1987**, *20*, 79.

(41) Farrugia, L. J. ORTEP-3. *J. Appl. Crystallogr.* **1997**, *30*, 565.

(42) Köhn, R. D.; Pan, Z.; Kociok-Köhn, G.; Mahon, M. F. *Dalton Trans.* **2002**, 2344.

(43) Bhattacharjee, R.; Jain, Y. S.; Bist, H. D. *J. Raman Spectrosc.* **1989**, *20*, 91.

(44) Moustiakimov, M.; Kritikos, M.; Westin, G. *Inorg. Chem.* **2005**, *44*, 1499.

(45) Li, W.; Wang, R.; Si, S.; Li, Y. *J. Mol. Struct.* **2004**, *694*, 27.

(46) Bataille, T.; Auffredic, J.-P.; Louer, D. *J. Mater. Chem.* **2000**, *10*, 1707.

(47) Obora, Y.; Ohta, T.; Stern, C. L.; Mark, T. J. *J. Am. Chem. Soc.* **1997**, *119*, 3745.

(48) Ganesan, M.; Gambarotta, S.; Yap, G. P. A. *Angew. Chem., Int. Ed.* **2001**, *40*, 766.

(49) Yann, B.; Marinella, M.; Jacques, P.; Mariyn, M. O. *J. Am. Chem. Soc.* **2002**, *124*, 9012.

(50) Xu, J.; Raymond, K. N. *Angew. Chem., Int. Ed.* **2000**, *39*, 2745.

(51) Westin, L. G.; Kritikos, M.; Caneschi, A. *Chem. Commun.* **2003**, 1012.

(52) Sun, C.-Y.; Jin, L.-P. *Polyhedron* **2004**, *23*, 2085.

(53) Louër, M.; Louër, D.; Delgado, A. L.; Martinez, O. G. *Eur. J. Solid State Inorg. Chem.* **1989**, *26*, 241.

(54) Davies, G. M.; Aarons, R. J.; Motson, G. R.; Jeffery, J. C.; Adams, H.; Faulkner, S.; Ward, M. D. *Dalton Trans.* **2004**, 1136.

(55) Voloshin, A. I.; Shavaleev, N. M.; Kazakov, V. P. *J. Lumin.* **2001**, *93*, 199.